Rabi-like vibrational coherence transfer in a hydrogen-bonded charge transfer material

Aaron S. Rury and Jahan M. Dawlaty

Phys. Rev. B **95**, 214309 — Published 29 June 2017

DOI: 10.1103/PhysRevB.95.214309

Rabi-like Vibrational Coherence Transfer in a Hydrogen-Bonded Charge Transfer Material

Aaron S. Rury† and Jahan M. Dawlaty*
University of Southern California, Los Angeles CA, 90089

We report ultrafast spectroscopic measurements of inter-site charge transfer in a single crystal of the hydrogen-bonded material quinhydrone showing anti-correlated dynamics of vibrational coherences at 172 and 216 cm^{-1}. To explain these coherent dynamics we derive a density matrix model in the presence of higher order electron-vibration coupling. Given the symmetry of vibrations calculated using density functional theory, the Huang-Rhys parameter of the Raman-active vibration found from spontaneous resonance light scattering measurements, and previously reported non-resonant impulsive stimulated Raman scattering measurements on quinhydrone, we restrict the density matrix model to 3 levels in the excited state of this material to simulate the observed dynamics with a density matrix approach. The close agreement between the experiment and our theoretical treatment leads us to conclude that the measured behavior corresponds to intermolecular Rabi-like oscillatory coherence transfer. These results provide foundational knowledge into the capability of functional organic materials to support quantum coherent transport of charge and energy as well as shed light on recent experimental and theoretical investigations of room temperature organic ferroelectrics.

I. INTRODUCTION

Two important dynamical effects were understood for simple systems immediately following the inception of quantum mechanics. First, there is interference between quantum states possessing a well-defined phase relationship. In time domain experiments, interference appears as oscillations at frequencies proportional to the energy difference between the involved states. One example is the dynamics of coherent vibrational wave packets formed after pulsed excitation in materials.[1–5] Second, the interaction of quantum states can drive oscillations in the states' populations. Rabi first discovered this effect for an interaction between the two-level system and an electromagnetic field.[6] For a resonant interaction the populations oscillate at a rate directly proportional to the interaction strength known as the Rabi frequency, Ω.

After almost 100 years since the introduction of these ideas, dynamical quantum systems remain topics of both fundamental and applied interest. In the context of organic materials, long-lived phase coherence and the interference of excitations have been experimentally reported in light harvesting centers[7–16] and polymers.[17,18] However, demonstrating definite dynamical effects of quantum coupling analogous to Rabi oscillations have not been reported.

Despite the intense interest in the quantum aspects of energy and charge transfer processes in biologically relevant and disordered organic materials, similar processes in crystalline organic materials using state-of-the-art experimental approaches remain unexplored. Crystalline materials formed from electron donor (D) and electron acceptor (A) molecules possess highly anisotropic optical and transport properties due to the spatial confinement of charge transfer to the direction along intermolecular D-A separation. Previous studies have shown that this confinement in organic charge transfer (CT) crystals leads to Luttinger liquid behavior,[19,20] metal-to-insulator transitions,[21] spin-Peierls transitions,[22] quantum phase transitions,[23] and cooperative proton-electron transfer.[24] This plethora of fascinating phenomena makes organic CT crystals invaluable laboratories to study the quantum dynamics of energy and charge transport.

In this study, we report ultrafast pump-probe measurements, numerical calculations, and analytical simulations demonstrating signatures of a quantum mechanism of excitation transfer in a room temperature crystal of the CT material quinhydrone: Rabi-like intermolecular transfer of vibrational coherences. We propose that the dynamics uncovered in this study result from a nonlinear electron-vibration interaction in the excited electronic state of quinhydrone that couples the amplitudes of vibrational coherences in an oscillatory manner.

Quinhydrone is a hydrogen-bonded co-crystal of the electron donor hydroquinone (HQ) and electron acceptor benzoquinone (BQ) arranged in a series of alternating D and A sites. Quinhydrone is an essential organic crystalline material since an intimate relationship between electron and proton transfer allows its simultaneous measurement of both electrochemical potentials and pH. In addition, studies have found that quinhydrone-like chromophores form in proteins that control electron transfer between the interior and exterior of living cells.[25] Perhaps most important to the applications of organic materials, there is remaining debate concerning the ability of hydrogen-bonded co-crystals of electron donor and acceptor molecules to stabilize in ferroelectric phases at room temperature.[26,27] Thus, characterizing coherent, quantum transfer mechanisms central to the behavior of quinhydrone will shed light on myriad processes in condensed matter and materials physics as well as chemistry and biology.

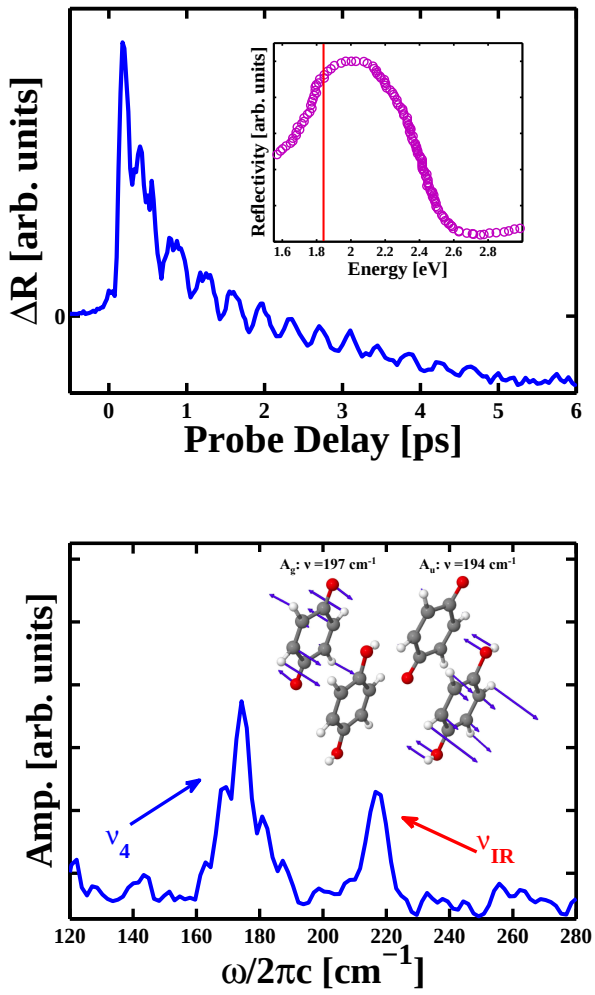

FIG. 1. Top: ultrafast transient reflectivity (TR) of a single monoclinic quinhydrone crystals following a pump pulse centered at 1.82 eV integrated over probe pulse energies from 1.3 eV to 1.7 eV. Top Inset: Comparison of previously reported steady-state reflectivity spectrum of monoclinic quinhydrone (purple circles) to the spectral position of the pump pulse (red line).[28] Bottom: Zoomed scale of the Fourier transformation of the integrated TR signal shown in the top panel indicating the coherent excitation of the ν_4 and ν_{IR} vibrations of quinhydrone by the pump pulse. Bottom Inset: Comparison of the atomic motions comprising an IR-active vibration found at 194 cm^{-1} (right) to those of a Raman-active vibration found at 197 cm^{-1} (left) calculated using density functional theory.

II. RESULTS AND DISCUSSION

Experimentally, we pump a monoclinic single crystal of quinhydrone on its CT resonance with a ∼50 fs pulse centered at 1.82 eV and probe the change in the reflectivity of the sample using a broadband white light continuum, as described previously.[29] The top inset of Figure 1 shows the spectral position of the pump pulse relative to the CT transition of quinhydrone reported previously for a reflection geometry.[28] The top panel of Figure 1 shows the ultrafast transient reflectivity signal integrated over probe energies from 1.29 eV to 1.7 eV, the region of this material's CT resonance.[5] The full 2-dimensional TR spectrum can be found in Figure S1 of the Supplemental Materials.[30] Oscillations in the transient reflectivity of the probe pulse correspond to the time evolution of coherent superpositions of vibrational quantum states impulsively excited by the resonant pump pulse. To facilitate analysis of these oscillations we have re-mapped the raw data of Figure S1 for pump-probe delays ranging from -4.8 ps to 12.5 ps onto a uniform gird of 10 fs time steps using linear interpolation and applied a singular value decomposition analysis detailed elsewhere.[5] Interpolation onto larger time steps cannot reliably reproduce the raw integrated transient reflectivity signal shown in the top panel of Figure 1.

Previously, Fourier transformation (FT) of similar time domain signals measured in quinhydrone has shown that the dominant contributions to these oscillations come from the intermolecular lattice vibrations below 300 cm^{-1}.[5,29,31] For this study, we consider the region of the signal FT corresponding to values between 120 cm^{-1} and 280 cm^{-1}. In this region a feature appears at 216 cm^{-1} which appears in neither the steady-state resonance Raman spectra of quinhydrone found in Figure S2 nor the FT of a non-resonantly excited ultrafast impulsive stimulated Raman scattering measurement reported previously and discussed below.[32]

Density functional theory (DFT) calculations detailed in the Supplemental Materials motivate the conclusion that the peak at 216 cm^{-1} corresponds to a vibration of quinhydrone. The DFT calculations find an A_u IR-active vibration at 194 cm^{-1} largely localized on the D site, HQ, in addition to an A_g Raman-active vibration at 197 cm^{-1} largely localized on the A site, BQ. The appearance of an IR-active vibration near 200 cm^{-1} is consistent with polarized far-IR absorption spectra of quinhydrone reported previously.[28] Given its activity, we will further refer to the 216 cm^{-1} vibration as ν_{IR} while we assign vibration at 197 cm^{-1} as ν_4, consistent with our previous work.[5] The inset of the bottom panel of Figure 1 shows the atomic motions comprising these two vibrations found from the DFT calculations.

The dynamics of the vibrational coherences also show interesting behavior. Figure 2 shows the spectrogram for frequencies that correspond to values between 135 cm^{-1} and 250 cm^{-1}. To uncover these dynamics, a FT is performed over a window 5.2 ps wide, which is swept by 10 fs steps across a total pump-probe delay time of 15 ps around the pump-probe temporal overlap. The resulting spectrogram shows the spectral density of coherences with the 5.2 ps window centered at each pump-probe delay. The appearance of both the ν_4 and ν_{IR} coherences at the same frequencies as found from the full FT shown in the bottom panel of Figure 1 supports the conclusion that the spectrogram accurately captures their dynamics.

In Figure 2 we see that the ν_4 coherence peaks with

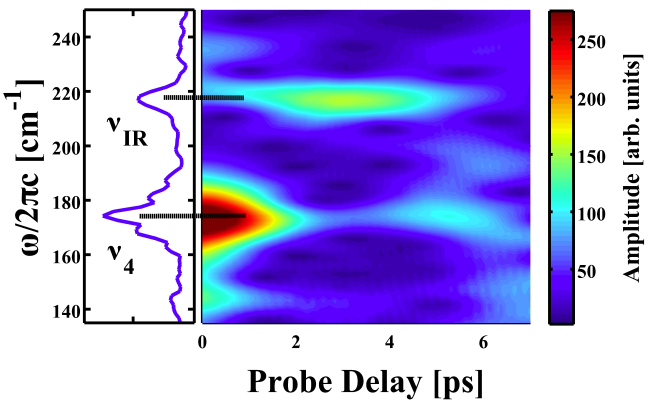

FIG. 2. Spectrogram of the integrated transient reflectivity signal measured from a single monoclinic quinhydrone crystal for Fourier frequencies corresponding to values between 135 cm^{-1} and 250 cm^{-1} following a pump pulse centered at 1.82 eV.

the temporal overlap of the pump and probe pulses and there is a delay in the peaking of the 216 cm^{-1} coherence. Furthermore, one sees that as the amplitude of the 216 cm^{-1} coherence reaches its peak, there is an associated minimum in the amplitude of the ν_4 coherence. Subsequently, the amplitude of the ν_4 coherence begins to increase as the 216 cm^{-1} coherence reduces. These features are consistent with *coherence transfer* processes in the ultrafast dynamics of quinhydrone[32–36]. In vibrational coherence transfer, a coherent superposition of quantum states along one vibration drives a similar coherent superposition along a different vibration.

In a previous study, we reported evidence for coherence transfer between a librational mode centered on the electron donor of quinhydrone, HQ, and an intramolecular vibration of the same crystalline site following nonresonant ultrafast electromagnetic excitation. We then used the frequency of intramolecular vibrational coherence to motivate a physical picture in which coherent lattice vibrations drive intermolecular charge transfer on ultrafast time scales. We did not, however, see the recurrence of the initial coherence of the librational mode following the decay of the intramolecular vibrational coherence. In contrast to this previous result, the anti-correlated behavior of the two coherence amplitudes of Figure 2 indicates resonant optical excitation drives a quantum coupling between these excitations of quinhydrone in which vibrational coherence *does* recur. To our knowledge, the results of Figure 2 differ from all previous reports of vibrational coherence transfer. Furthermore, the DFT calculations highlighted above indicate that the resonantly-driven quantum coupling initiates intermolecular vibrational coherence transfer from the BQ site to the HQ site.

To test the reality of the results in Figure 2, we undertook two separate validation methods. In the first we calculated the spectrogram of the wave form in Figure 1 for several different window widths. Figure S3 shows that for window widths ranging from 3 ps to 5.12 ps we observe no difference in the temporal position of the minimum of the 172 cm^{-1} coherence amplitude nor the peak of the 216 cm^{-1} coherence amplitude. Based on this analysis, the anti-correlated behavior in the coherence amplitudes does not stem from the time window width chosen for the results shown in Figure 2.

In the second method, we convolved a Gaussian spike possessing a full width half maximum of 25 fs with both a exponential decay of 10 ps and two cosine waves of frequencies corresponding to values of 172 cm^{-1} and 216 cm^{-1}. We do not introduce any interaction between the two cosine waves. The resulting wave form shows significant beating between the two frequencies, as seen in the top panel of Figure 3. Despite these beating features, when we apply the same spectrogram algorithm to the model wave form as was applied to the measured wave form of quinhydrone we find no signatures of a time-dependent interaction between the amplitudes of each oscillatory feature, i.e. no coherence transfer. This conclusion is established in the bottom panel of Figure 3, which compares the time-integrated FT of the model wave form to the dynamics of the oscillatory amplitudes. Figure 3 shows no coupling behavior between the model oscillations, but rather only the dephasing of each oscillatory feature with its associated decay time. Based on these two methods, we conclude that the features of Figure 2 correspond to real physics occurring in quinhydrone on ultrafast time scales.

The experimental results of Figures 1 and 2 indicate that an interaction drives coherence transfer between Q_4 and Q_{IR} following ultrafast resonant excitation of quinhydrone. Recently, Rury has shown that a second order perturbative correction to the electronic Hamiltonian of quinhydrone due to lattice vibrations can drive interactions between excitations of different symmetry.[37] In that case, nonlinear electron-phonon coupling can explain Fano-like line shapes of these vibrational excitations in the spontaneous resonance Raman spectra of quinhydrone excited in the visible region.

One approach to understand the role of nonlinear electron-vibration (e-v) contributions that manifest themselves in the coherent vibrational dynamics is to develop a theory based on coherent state representation, as has been done previously for inorganic semiconductors.[38] To undertake this approach one must have a specific Hamiltonian to which nonlinear e-v coupling contributes, such as the extended Holstein-Peierls-Hubbard Hamiltonian.[37] As explained below, however, from the data we have accumulated at present it is not clear to which parts of the electronic Hamiltonian (on-site energy, intra-site electron correlation, or intermolecular charge transfer) vibrations couple as a second order perturbation. As such, one would need to guess the correct form of the second order correction to the system's energy to complete the theoretical treatment in the coherent state representation. Instead of taking such an approach without the necessary information at hand, we

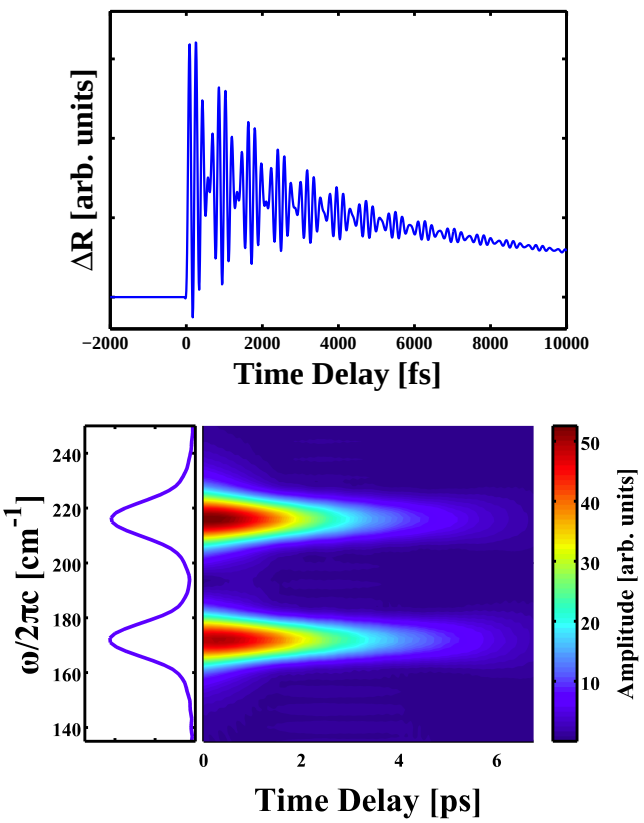

FIG. 3. Top: model wave form constructed from a convolution of a Gaussian spike with an exponential decay and two oscillations at frequencies corresponding to 172 cm^{-1} and 216 cm^{-1}. Bottom: comparison of the integrate Fourier transformation of the wave form shown in the top panel to its spectrogram for Fourier frequencies corresponding to values between 135 cm^{-1} and 280 cm^{-1} showing no interaction between isolated cosine oscillatory components inserted at 172 cm^{-1} and 216 cm^{-1}.

theoretically probe whether a higher order e-v mechanism can explain the results in Figure 1 and 2 using a density matrix approach.[39] The density matrix approach also highlights the similarities between our results and Rabi oscillations observed the interaction of two-level systems with electromagnetic radiation.

To simulate the dynamics with the density matrix, we model the charge-localized state, $|L\rangle$ and the charge-separated state, $|CT\rangle$, as multidimensional harmonic potential energy surfaces (PESs) with respect to both the ν_4 normal coordinate, Q_4, and the ν_{IR} normal coordinate, Q_{IR}, as shown in the top panel Figure 4. In this model, the $|CT\rangle$ PES is displaced along the Q_4, but not along Q_{IR}, in accordance with steady-state resonance Raman measurements shown in Figure S2 and reported previously.[29] Three points of the analysis allow further simplification of this model. First, the vibrations of interest to us possess frequencies that correspond to wavenumber values of 172 and 216 cm^{-1}, as shown by Figures 1 and 2. Therefore, the evidence for the contribution of coherences between quantum states of either vibration lying above the first excited state would be prominent features at the frequency difference between the involved vibrations. Throughout our analysis we have not been able to isolate a distinct feature in either the time-integrated FT or the spectrogram at either the difference or multiples of the difference between $\omega_{IR}/2\pi c$ and $\omega_4/2\pi c$.

Second, as shown in Figure S2, there is no evidence of the overtone of the ν_4 mode in the spontaneous Raman scattering measurements excited at 2.33 eV. The lack of an overtone signature indicates that the Huang-Rhys parameter for ν_4 upon excitation to $|CT\rangle$ must be sufficiently small that only the ground and first excited vibrational states possess sizable Franck-Condon overlap integrals between the electronic state $|L\rangle$ and $|CT\rangle$.

Third, as seen in our previous studies, non-resonant impulsive stimulated Raman scattering (ISRS) excitation of a quinhydrone single crystal at 0.95 eV induces vibrational coherences whose amplitude and dynamics significantly differ from those found in Figures 1 and 2.[5,32] These differences have been used to conclude that non-resonant ISRS excitation definitively drives vibrational coherences in the ground electronic state of quinhydrone, $|L\rangle$. In addition, while ISRS excitation drives coherences of the ν_4 mode, there is no evidence that this light-matter interaction drives ν_{IR}. Based on these considerations, we conclude that a coherent superposition of states along ν_{IR} mode froms through excitation to the excited state of quinhydrone, $|CT\rangle$. We can use the probe energy dependence of the ν_{IR} to determine if the coherent excitation of the ν_{IR} mode remains in $|CT\rangle$ following coherence transfer.

Unlike incoherent vibrational excitation often driven by a thermal bath, vibrational coherences produce non-zero, average displacements of the atoms along each associated normal coordinate.[38] These atomic displacements can then change the energy necessary to make an electronic transition. By spectrally resolving the amplitude and phase of a vibrational coherence we can assess its coupling to any electronic transitions resonant with the probe pulse, as detailed by several authors.[5,31,40–43] The electron-vibration coupling manifests itself in the resultant quantity, which we call the vibrational coherence spectrum (VCS), as a dip in the amplitude and shift in the phase of vibrational coherence centered at the peak of the electronic transition.

Figure 5 compares the VCS of ν_4 following non-resonant ISRS excitation at 0.95 eV to that of ν_{IR} taken from the measurements detailed above. The most conspicuous difference between these spectra is the lack of a significant amplitude dip and associated phase shift of the ν_{IR} coherence near 1.68 eV, which is seen clearly in the top panel for the ν_4 mode in quinhydrone's ground state. Previously we had used the VCS of several vibrational coherences to assign this feature as the CT band edge.[32] Given the modulation of the aromatic ring atomic positions by ν_{IR} found from DFT calculations shown in the bottom inset of Figure 1, it seems unlikely that ν_{IR}

would not modulate the CT gap energy upon its coherent excitation in the ground state of quinhydrone. The most likely explanation for the lack of a distinct feature at 1.68 eV in the VCS of ν_{IR} is that the resonant excitation drives this vibrational coherence in $|CT\rangle$ and the vast majority of its coherent amplitude remains in that electronic state throughout its evolution.

Therefore, based on these three points we conclude that we can extract three vibrational levels in $|CT\rangle$ from the full model of PESs to efficiently simulate the observed dynamics. The bottom panel of Figure 4 shows these essential states where the levels $|1\rangle$, $|2\rangle$, and $|3\rangle$ correspond to the ground, singly excited ν_4, and singly excited ν_{IR} states in $|CT\rangle$, respectively.

With the states we believe to be essential to modeling the dynamics of quinhydrone, we can construct a density matrix model based on nonlinear e-v coupling to simulate the results of Figure 2. In the specific case of ν_4 and ν_{IR} we write the nonlinear e-v coupling interaction as

$$\hat{H}^{(2)}_{e-v} = \left(\frac{\partial^2 \hat{H}_e}{\partial Q_4 \partial Q_{IR}}\right)_{eq} Q_4 Q_{IR}, \tag{1}$$

where the second derivative of the electronic Hamiltonian of the material, $\hat{H}_e$, with respect to Q_4 and Q_{IR} is the nonlinear e-v coupling constant. To further highlight the dynamics important to the results of Figures 1 and 2, we use the interaction picture. In the interaction picture, the density matrix obeys the relation $\frac{d\hat{\rho}_I}{dt} = \frac{-\imath}{\hbar}[\hat{V}_I(t), \hat{\rho}_I(t)]$.[44] In our case of nonlinear e-v coupling, the coherence amplitudes $\rho_{12}(t)$ and $\rho_{13}(t)$ obey the set coupled differential equations,

$$\frac{d\rho_{12}}{dt} = \frac{-i\langle 2|\hat{H}^{(2)}_{e-v}(t)|3\rangle}{\hbar}\rho_{13}(t), \tag{2a}$$

$$\frac{d\rho_{13}}{dt} = \frac{-i\langle 3|\hat{H}^{(2)}_{e-v}(t)|2\rangle}{\hbar}\rho_{12}(t), \tag{2b}$$

where the subscript, I, has been omitted for brevity. Inspection of Eq. (2a) ($Eq.(2b)$) shows that the coherence $\rho_{12}(t)$ ($\rho_{13}(t)$) will only evolve in the interaction picture when the matrix element $\langle 2|\hat{H}^{(2)}_{e-v}(t)|3\rangle$ $\left(\langle 3|\hat{H}^{(2)}_{e-v}(t)|2\rangle\right)$ is non-zero. This condition will be met when Q_4 and Q_{IR} couple together to modulate the electronic Hamiltonian and one takes the contributions to Eq. (1) that mix the creation of a vibrational excitation of one mode with an annihilation of a vibrational excitation of its counterpart.

While the form of Eq. (1) is typically useful for equilibrium and steady-state situations, our measurement occur under non-equilibrium conditions. Thus, we must propose a time-dependent form of Eq. (1) to insert in Eqs. (2a) and (2b). Since our measurements are sensitive to the ultrafast changes in the strength of the coupling of electrons and vibrations in quinhydrone, we propose the nonlinear e-v interaction must take time to

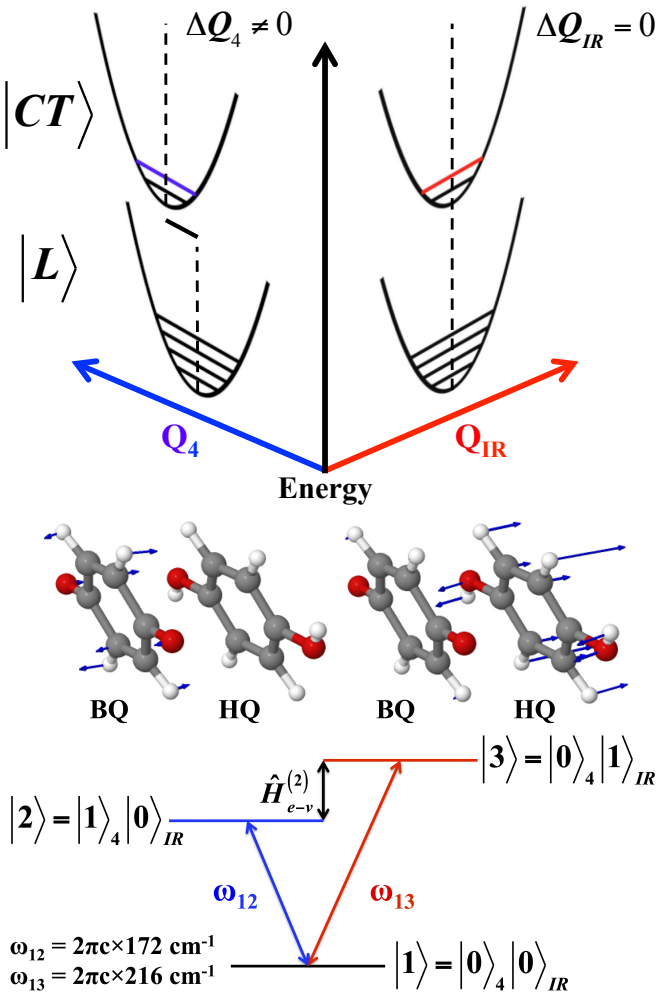

FIG. 4. Top: Model schematic of the potential energy surfaces of the charge-localized state, $|L\rangle$, and charge-separated state, $|CT\rangle$, of quinhydrone with respect to the normal coordinates of ν_4 (blue) and ν_{IR} (red). Bottom: Schematic of the three level model of vibrational eigenstates of quinhydrone in $|CT\rangle$ coupled by the nonlinear electron-vibrational interaction $\hat{H}^{(2)}_{e-v}$ used to simulate the experimental dynamics. The first excited states of ν_4 and ν_{IR} colored-coded in the same manner as the top panel and are shown on the left and right, respectively, with their associated atomic motions derived from DFT calculations.

'turn-on' and then will decay as the electronic population in $|CT\rangle$ relaxes. A rise time in the interaction between the two vibrations is physically reasonable since the nuclei of the crystal cannot respond instantaneously to the change in electronic structure induced by the pump pulse. Furthermore, when we drive a coherent amplitude along the ν_4 and ν_{IR} vibrations, their associated normal coordinates become oscillatory in time and interfere. Based on these considerations, we proposed that the time-dependent nonlinear e-v interaction can be written

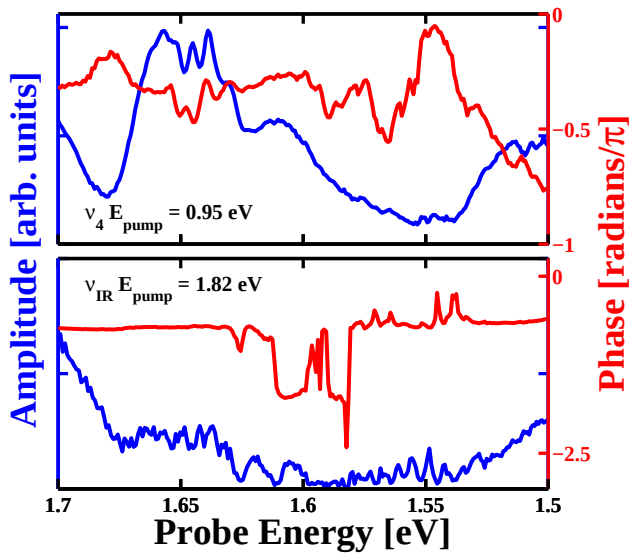

FIG. 5. (color online) Top: vibrational coherence spectrum of the ν_4 mode of quinhydrone found at 172 cm^{-1} following electronically non-resonant impulsive stimulated Raman scattering excitation at 0.95 eV. Bottom: vibrational coherence spectrum of the ν_{IR} mode of quinhydrone found at 216 cm^{-1} following electronically resonant excitation at 0.95 eV.

as,

$$\hat{H}^{(2)}_{e-v}(t) = \left(\frac{\partial^2 \hat{H}_e(t)}{\partial Q_4 \partial Q_{IR}}\right) e^{\imath\omega t} \tag{3}$$
$$= \left(\frac{\partial^2 \hat{H}_e}{\partial Q_4 \partial Q_{IR}}\right)_0 \sqrt{\frac{t}{t_1}} e^{-t/t_2} e^{\imath\omega t},$$

where t_1 characterizes the rise of the interaction in $|CT\rangle$ and t_2 characterizes its decay on longer time scales. We note that the subscript on the coupling constant in the second line of Eq. (3) is not necessarily equivalent to the subscript on the coupling constant in Eq. (1).

As a first order attempt to model the dynamics of Figure 2, we do not consider the time dependence of $\left(\frac{\partial^2 \hat{H}_e(t)}{\partial Q_j \partial Q_l}\right)$ in solving Eqs. (2a) and (2b). We also add phenomenological dephasing rates Γ_{12} and Γ_{13} for $\rho_{12}(t)$ and $\rho_{13}(t)$ coherences, respectively, and add a baseline due to the decaying tail of any lower energy excitations in the spectrogram that decays with a time constant t_d. With these assumptions and taking the rotating wave approximation, the modeled coherence amplitudes take the form,

$$\rho_{12}(t) = A_{12} e^{-t/t_d} \tag{4a}$$
$$+ e^{-\Gamma_{12} t} e^{\imath\Delta t/2} \left[\cos\frac{\Omega(t)t}{2} - \frac{\imath\Delta}{\Omega(t)} \sin\frac{\Omega(t)t}{2}\right],$$
$$\rho_{13}(t) = A_{13} e^{-t/t_d} \tag{4b}$$
$$+ e^{-\Gamma_{13} t} e^{\imath\Delta t/2} \frac{2\imath\gamma(t)}{\hbar\Omega(t)} \sin\frac{\Omega(t)t}{2},$$

where $\gamma(t) = \langle 3| \left(\frac{\partial^2 \hat{H}_e(t)}{\partial Q_4 \partial Q_{IR}}\right) |2\rangle$, $\Delta = \omega - (\omega_{13} - \omega_{12})$, and $\Omega(t) = \sqrt{\Delta^2 + \frac{4|\gamma(t)|^2}{\hbar^2}}$. The form of Eqs. (4a) and (4b) are similar to the solution to Rabi's original problem.[6] For instance, our model predicts that in the presence of an interaction, $\rho_{12}(t)$ and $\rho_{13}(t)$ will oscillate in amplitude at a frequency of $\Omega(t)$. However, two features distinguish Eqs. (4a) and (4b) from Rabi's original analysis. First, instead of an interaction between two states and an electromagnetic (EM) field, we propose that nonlinear e-v coupling in quinhydrone drives the dynamics of our analysis. Second, we examine the dynamics of vibrational coherences instead of the populations typically studied in the interaction of a two-level system with an EM-field. Despite these differences, we find our problem of two coherences interacting via nonlinear e-v coupling closely resembles that of two populations interacting via an EM field on a fundamental level.

Figure 6 compares the experimental dynamics of the coherence amplitudes at 172 and 216 cm^{-1} to the model using Eqs. (4a) and (4b). The bottom panel of Figure 6 shows the results of the calculation when $\rho_{12}(0) = 1$ and we use $\left(\frac{\partial^2 \hat{H}_e}{\partial Q_4 \partial Q_{IR}}\right)_0 = 0.90$ meV, $\hbar\Delta = 0.6$ meV, $\hbar\Gamma_{12} = 0.09$ meV, and $\hbar\Gamma_{13} = 0.12$ meV. The simulation shown in Figure 6 uses rise and decay time constants of 0.2 ps and 9.5 ps corresponding to the vibrational period of the ν_4 and electronic relaxation probed in the near-IR, respectively.[29] t_d was set to 10 ps while A_{12} and A_{13} are 0.1 and 0.05. Comparison of the top and bottom panels of Figure 6 shows that the density matrix dynamics of the 3-level model capture the qualitative behavior of the experimental data well, even without explicitly accounting for the time dependence of the interaction strength, $\left(\frac{\partial^2 \hat{H}_e(t)}{\partial Q_j \partial Q_l}\right)$. The remaining quantitative disagreement between theory and experiment likely stems from this approach. Nevertheless, based on Figure 6 we tentatively conclude that the amplitudes of the ν_4 and ν_{IR} vibrational coherences undergo oscillations due to nonlinear e-v coupling in the charge separated state of this material, i.e. Rabi-like coherence oscillations.

While the interaction in Eq. (1) has provided the correct form to explain the anti-correlated dynamics of ν_4 and ν_{IR} in quinhydrone, it is not entirely clear to which part of the electronic Hamiltonian these vibrations couple. However, arguing that only quantum vibrational states in the $|CT\rangle$ of quinhydrone participate in the coherence transfer process, we have presumed that intermolecular charge transfer does not play a significant role.

Previously, several authors have considered the anharmonic coupling of intra- and intermolecular vibrations in the co-crystal of tetrathiafulvalene (TTF) and chloranil (CA) mediated by charge transfer between the donor and acceptor sites of this material. The broad interest in TTF-CA stems from its ability to stabilize in a ferroelectric electronic phase following charge transfer driven by several types of external stimuli.[45–50] When driven by sufficiently short pulses of resonant EM radiation,

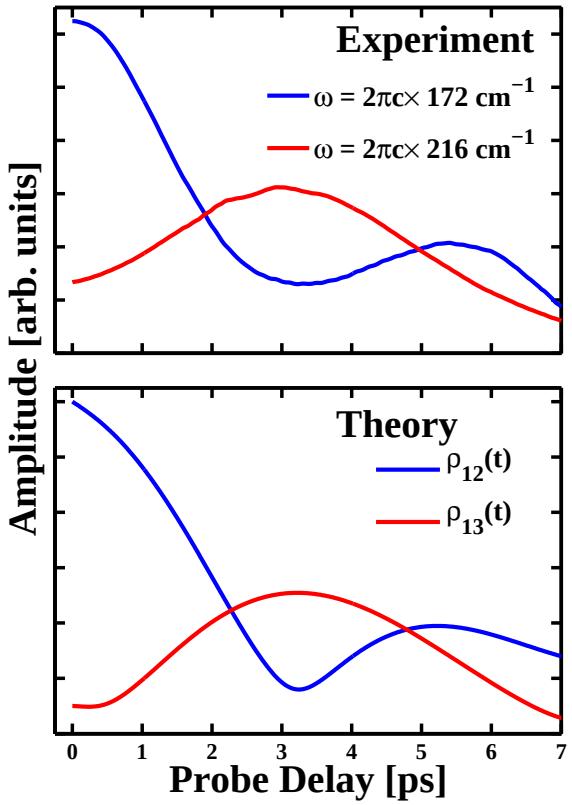

FIG. 6. (color online) Top: comparison of the dynamics of the coherence measured at 172 cm^{-1} to those measured at 216 cm^{-1} clearly showing the anti-correlated dynamical behavior. Bottom: comparison of the dynamics of model vibrational coherence ρ_{12} (blue) to those of ρ_{13} (red) found from analytical modeling using method described in the text. The qualitative agreement between the two panels indicates that an interaction drives ultrafast Rabi-like coherence transfer between the vibrational states of Figure 4.

one observes frequency modulation of an intramolecular vibration of TTF by the Peierls mode of this material near 50 cm^{-1}.[50,51] To explain this and other phenomena in TTF-CA, Painelli, Zoos, and co-workers have developed a theory of coupled diabatic PESs that couple both intra- and intermolecular vibrations to charge transfer.[51–53] This is a powerful method to explain the vibration-vibration coupling mediated by collective electronic effects in a strongly correlated material and has been used to benchmark a theoretical approach to asses claims of ferroelectricity in supramolecular hydrogen-bonded charge-transfer complexes.[26,27]

From the experimental evidence amassed thus far, it is not clear that similar collective electronic phenomena also take part in the ultrafast dynamics of quinhydrone. For instance, we have not found evidence of a Peierls mode in quinhydrone. In addition, the ν_4 and ν_{IR} modes of quinhydrone are separated by a significantly smaller frequency difference than the vibrations that couple in TTF-CA. Nonetheless, it would be interesting to explore whether the theoretical approach taken by Painelli, Zoos, and co-workers could explain the coherent transfer of vibrational excitation in quinhydrone. However, such an approach may have to differ to a meaningful degree from that already taken to asses room temperature ferroelectricity. This caution arises from the fact that it seems the data presented above are not consistent with a charge transfer mechanism driving the coupling between ν_4 and ν_{IR} that leads to coherence transfer. While a treatment similar to that developed Painelli, Zoos, and co-workers is beyond the scope of the current study, the results presented above would provide the first dynamical results testable with such a theoretical approach in the case of a hydrogen-bonded charge transfer crystal. Such a treatment would provide a clearer picture of the ability of hydrogen-bonded charge transfer materials to attain electronic phases functional for next generation technologies.

III. CONCLUSIONS

We have used the experimental and theoretical dynamics of coherences to motivate the conclusion that a nonlinear electron-vibration interaction drives the coupling of vibrations on the donor and acceptor sites of the hydrogen-bonded charge-transfer material quinhydrone on ultrafast timescales. Analytical modeling shows that this coupling manifests itself as Rabi-like oscillations in the amplitudes of vibrational coherences. We used vibrational coherence spectroscopy to conclude that this transfer process occurs in the charge-separated excited state of quinhydrone. This conclusion is especially important since recent theoretical results derived from a theoretical Hamiltonian using terms including the anharmonic coupling of intra- and intermolecular vibrations mediated by intermolecular charge transfer have cast doubt on the ability of hydrogen-bonded charge-transfer materials to achieve spontaneous ferroelectric phases at room temperature. Our results and analysis show that one needs to asses the contributions of additional anharmonic corrections to the electronic Hamiltonians to more completely understand the properties of this new class of supramolecular materials.

ACKNOWLEDGMENTS

The authors acknowledge support from the University of Southern California start up grant and the AFOSR YIP Award (FA9550-13-1-0128). ASR was partially supported by the Rose Hills Foundation Research Fellowship. JMD was partially supported by the NSF CAREER Award (1454467). The authors thank Duncan Steel, Jennifer Ogilvie, Steven Cundiff, and Evgeniia Butaeva for useful feedback and encouragement and Dr. Jon Dieringer, Eric Driscoll, and Shayne A. Sorenson for contributions to the development of the software used in the

reported ultrafast spectroscopic measurements.

* †arury@usc.edu; *dawlaty@usc.edu

[1] H. J. Zeiger, J. Vidal, T. K. Cheng, E. P. Ippen, G. Dresselhaus, and M. S. Dresselhaus, Phys. Rev. B **45**, 768 (1992).
[2] L. Dhar, J. A. Rogers, and K. A. Nelson, Chem. Rev. **94**, 157 (1994).
[3] R. Merlin, Solid State Commun. **102**, 207 (1997).
[4] L. Lüer, C. Gadermaier, J. Crochet, T. Hertel, D. Brida, and G. Lanzani, Phys. Rev. Lett. **102**, 127401 (2009).
[5] A. S. Rury, S. Sorenson, E. Driscoll, and J. M. Dawlaty, J. Phys. Chem. Lett. **6**, 3560 (2015).
[6] I. I. Rabi, Phys. Rev. **51**, 652 (1937).
[7] G. S. Engel, T. R. Calhoun, E. L. Read, T.-K. Ahn, T. Mancal, Y.-C. Cheng, R. E. Blankenship, and G. R. Fleming, Nature **446**, 782 (2007).
[8] H. Lee, Y.-C. Cheng, and G. R. Fleming, Science **316**, 1462 (2007).
[9] J. M. Womick and A. M. Moran, J. Phys. Chem. B **113**, 15747 (2009).
[10] E. Collini, C. Y. Wong, K. E. Wilk, P. M. G. Curmi, P. Brumer, and G. D. Scholes, Nature **463**, 644 (2010).
[11] V. Tiwari, W. K. Peters, and D. M. Jonas, Proc. Natl. Acad. Sci. U.S.A. **110**, 1203 (2013).
[12] S. D. McClure, D. B. Turner, P. C. Arpin, T. Mirkovic, and G. D. Scholes, J. Phys. Chem. B **118**, 1296 (2014).
[13] F. D. Fuller, J. Pan, A. Gelzinis, V. Butkus, S. S. Senlik, D. E. Wilcox, C. F. Yocum, L. Valkunas, D. Abramavicius, and J. P. Ogilvie, Nat. Chem. **6**, 706 (2014).
[14] J. E. Donehue, O. P. Varnavski, R. Cemborski, M. Iyoda, and T. Goodson, J. Am. Chem. Soc. **133**, 4819 (2011).
[15] D. Hayes, G. B. Griffin, and G. S. Engel, Science **340**, 1431 (2013).
[16] J. Lim, D. Paleček, F. Caycedo-Soler, C. N. Lincoln, J. Prior, H. von Berlepsch, S. F. Huelga, M. B. Plenio, D. Zigmantas, and J. Hauer, Nat. Commun. **6**, 7755 (2015).
[17] N. P. Wells and D. A. Blank, Phys. Rev. Lett. **100**, 086403 (2008).
[18] S. M. Falke, C. A. Rozzi, D. Brida, M. Maiuri, M. Amato, E. Sommer, A. De Sio, A. Rubio, G. Cerullo, E. Molinari, and C. Lienau, Science **344**, 1001 (2014).
[19] A. Schwartz, M. Dressel, G. Grüner, V. Vescoli, L. Degiorgi, and T. Giamarchi, Phys. Rev. B **58**, 1261 (1998).
[20] F. Zwick, D. Jérome, G. Margaritondo, M. Onellion, J. Voit, and M. Grioni, Phys. Rev. Lett. **81**, 2974 (1998).
[21] A. J. Epstein, S. Etemad, A. F. Garito, and A. J. Heeger, Phys. Rev. B **5**, 952 (1972).
[22] I. S. Jacobs, J. W. Bray, H. R. Hart, L. V. Interrante, J. S. Kasper, G. D. Watkins, D. E. Prober, and J. C. Bonner, Phys. Rev. B **14**, 3036 (1976).
[23] S. Horiuchi, Y. Okimoto, R. Kumai, and Y. Tokura, Science **299**, 229 (2003).
[24] T. Mitani, G. Saito, and H. Urayama, Phys. Rev. Lett. **60**, 2299 (1988).
[25] J. Regeimbal, S. Gleiter, B. L. Trumpower, C.-A. Yu, M. Diwakar, D. P. Ballou, and J. C. A. Bardwell, Proc. Natl. Acad. Sci. U.S.A. **100**, 13779 (2003).
[26] A. S. Tayi, A. K. Shveyd, A. C.-H. Sue, J. M. Szarko, B. S. Rolczynski, D. Cao, T. J. Kennedy, A. A. Sarjeant, C. L. Stern, W. F. Paxton, W. Wu, S. K. Dey, A. C. Fahrenbach, J. R. Guest, H. Mohseni, L. X. Chen, K. L. Wang, J. F. Stoddart, and S. I. Stupp, Nature **488**, 485 (2012).
[27] G. D'Avino and M. J. Verstraete, Phys. Rev. Lett. **113**, 237602 (2014).
[28] T. Mitani and G. Saito, Syn. Met. **27**, B499 (1988).
[29] A. S. Rury, S. Sorenson, and J. M. Dawlaty, J. Chem. Phys. **144**, 104701 (2016).
[30] "See supplemental material at for the 2-dimensional transient reflectivity spectrum of quinhydrone, description of density functional calculations undertaken to determine vibrational spectrum of quinhydrone, a resonance raman spectrum of quinhydrone excited at 2.33 ev in the spectral region of 130 cm^{-1} to 365 cm^{-1}, and comparisons of the dynamics of vibrational coherences at 172 cm^{-1} and 216 cm^{-1} found from spectrogram calculations using different hamming window widths.".
[31] A. S. Rury, S. A. Sorenson, and J. M. Dawlaty, J. Phys. Chem. C **120**, 21740 (2016).
[32] A. S. Rury, S. A. Sorenson, and J. M. Dawlaty, J. Phys. Chem. Lett. **8**, 181 (2017).
[33] M. Khalil, N. Demirdöven, and A. Tokmakoff, J. Chem. Phys. **121**, 362 (2004).
[34] A. V. Pakoulev, M. A. Rickard, K. A. Meyer, K. Kornau, N. A. Mathew, D. E. Thompson, and J. C. Wright, J. Phys. Chem. A **110**, 3352 (2006).
[35] M. J. Nee, C. R. Baiz, J. M. Anna, R. McCanne, and K. J. Kubarych, J. Chem. Phys. **129**, 084503 (2008).
[36] C. R. Baiz, K. J. Kubarych, and E. Geva, J. Phys. Chem. B **115**, 5322 (2011).
[37] A. S. Rury, Phys. Rev. B **93**, 214307 (2016).
[38] A. V. Kuznetsov and C. J. Stanton, Phys. Rev. Lett. **73**, 3243 (1994).
[39] U. Fano, Rev. Mod. Phys. **29**, 74 (1957).
[40] A. T. N. Kumar, F. Rosca, A. Widom, and P. M. Champion, The Journal of Chemical Physics **114**, 701 (2001).
[41] A. T. N. Kumar, F. Rosca, A. Widom, and P. M. Champion, The Journal of Chemical Physics **114**, 6795 (2001).
[42] V. Karunakaran, Y. Sun, A. Benabbas, and P. M. Champion, J. Phys. Chem. B **118**, 6062 (2014).
[43] J. A. Cina, P. A. Kovac, C. C. Jumper, J. C. Dean, and G. D. Scholes, The Journal of Chemical Physics **144**, 175102 (2016).
[44] A. Nitzan, *Chemical Dynamics in Condensed Phases* (Oxford University Press, New York, NY, 2013).
[45] J. B. Torrance, J. E. Vazquez, J. J. Mayerle, and V. Y. Lee, Physical Review Letters **46**, 253 (1981).
[46] J. B. Torrance, A. Girlando, J. J. Mayerle, J. I. Crowley, V. Y. Lee, P. Batail, and S. J. LaPlaca, Phys. Rev. Lett. **47**, 1747 (1981).
[47] M. H. Lemée-Cailleau, M. Le Cointe, H. Cailleau, T. Luty, F. Moussa, J. Roos, D. Brinkmann, B. Toudic, C. Ayache, and N. Karl, Phys. Rev. Lett. **79**, 1690 (1997).
[48] S. Koshihara, Y. Takahashi, H. Sakai, Y. Tokura, and T. Luty, The Journal of Physical Chemistry B **103**, 2592 (1999).

[49] H. Okamoto, Y. Ishige, S. Tanaka, H. Kishida, S. Iwai, and Y. Tokura, Physical Review B **70**, 165202 (2004).
[50] H. Uemura and H. Okamoto, Phys. Rev. Lett. **105**, 258302 (2010).
[51] L. Cavatorta, A. Painelli, and Z. G. Soos, Phys. Rev. B **91**, 174301 (2015).
[52] Z. G. Soos, S. A. Bewick, A. Peri, and A. Painelli, J. Chem. Phys. **120**, 6712 (2004).
[53] A. Painelli and Z. G. Soos, Chem. Phys. **325**, 48 (2006).